

Bimetallic Gold–Silver Nanorods Produce Multiple Surface Plasmon Bands

Sungwan Kim,[†] Seong Kyu Kim,^{*,†} and Sungho Park^{*,†,‡,§}

Departments of Chemistry and Energy Science and SKKU Advanced Institute of Nanotechnology,
Sungkyunkwan University, Suwon 440-746, South Korea

Received April 17, 2009; E-mail: skkim@skku.edu (Seong Kyu Kim); spark72@skku.edu (Sungho Park)

Collective oscillation of loosely bound electrons on a metal surface can be induced by incident light waves that satisfy the electrons' resonance condition.¹ Specifically, the charge density oscillations of metals on a nanometer scale are referred to as localized surface plasmons (LSPs). The control of LSPs is a key feature that dictates the performance of nanoscale optic and photonics devices, as well as the fabrication of biosensors.^{2,3} When the frequency of incident light meets the resonance condition of nanoparticles, distinctive LSP absorption bands (i.e., bands of unique color) appear. The resonance condition depends on the size, shape, composition, and dielectric constants of the metal and the surrounding medium.³ It is known that nanorods (NRs) display transverse and longitudinal modes that oscillate along both the short and long axes, respectively.⁴ When NRs are physically larger than a certain limit ($L \geq 250$ nm, when $D \approx 80$), higher-order LSP modes can be observed.^{5,6} Herein, we report intraparticle surface plasmon coupling in NRs composed of a sequential array of nanofabricated Au–Ag blocks. We observed two independent transverse modes from the Au and Ag blocks. Depending on the relative fraction of Au and Ag blocks, the intensity of the transverse modes varied without noticeable peak shifts. However, the strong intraparticle surface plasmon coupling resulted in the collective appearance of longitudinal LSP modes, including higher-order modes.

Homogeneous and multiblock NRs of Au and Ag with diameters of 83 (± 5) nm and up to ~ 560 μm in length were synthesized by potentiostatic electrochemical deposition in anodized aluminum oxide templates. The diameter of the NRs was determined by the template pore size, while the length was tailored by adjusting the total charge passed through the electrochemical cell.⁷ After dissolving the templates and the subsequent release of the NRs into solution, the optical properties of colloidal suspensions of these nanostructures were characterized. The lengths of all investigated NRs were fixed to ca. 560 nm to observe higher-order modes of longitudinal LSPs, and the lengths of Ag blocks were varied systematically from 100, 160, 240, and 380 nm as shown in panels A–D of Figure 1, respectively. Typical field-emission scanning electron microscopy (FESEM) images of Au–Ag multiblock NRs showed that individual NRs had a fairly homogeneous size and block distribution. The size distributions of the total length and block length were within 10% of the average length. A careful inspection of FESEM images allowed us to differentiate the two bright Au ends from the dark Ag center block due to subtle differences in the energy of ejected secondary electrons. The corresponding UV–vis–NIR spectra of the NRs are presented in panel E. The spectrum of pure Au NRs with physical dimensions comparable to those of Au/Ag NRs is plotted with a red line. The band at ca. 550 nm can be assigned to a transverse LSP mode, and the broad feature at 1140 nm, to a quadrupole longitudinal LSP mode. The longitudinal dipole mode shifted beyond the investigated spectrum (~ 1800 nm) window and only showed a trace of a tail around 1800 nm. The

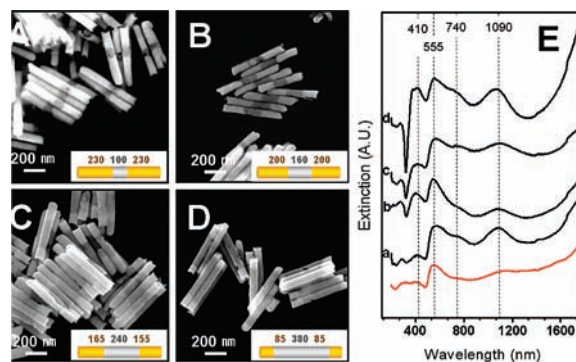


Figure 1. FESEM images of multiblock Au/Ag NRs (diameter ~ 83 (± 5) nm). Total average lengths are (A) 560 (± 56) nm, (B) 560 (± 57) nm, (C) 560 (± 40), and (D) 550 (± 37) nm. The insets show the dimensions of each block, yellow color for Au and gray for Ag, where the numbers represent the length in nanometer. (E) Visible–near IR extinction spectra corresponding to the FESEM images. The spectrum (a) was obtained from the sample shown in image (A), (b) to (B), (c) to (C), and (d) to (D), respectively. The red solid line is the experimental spectrum for the single-component Au NRs with a total length of 580 (± 68) nm. All spectra were unnormalized and measured in D_2O .

spectrum of Au (230 nm)–Ag (100 nm)–Au (230 nm) multiblock NRs (Figure 1A) is represented by trace *a* in panel E. The spectrum is very similar to that of pure Au NRs. The appearance of a clear band at 1090 nm as well as the long tail beyond 1600 nm reveals strong LSP coupling in the long axis between the Au and Ag blocks. The band at 740 nm can be assigned to a higher-order longitudinal LSP mode. This clear band emphasizes the effective intraparticle coupling in a heterogeneous NR. Another noticeable feature was the appearance of a band at 410 nm. In single-component Au NRs, there is no band visible at this wavelength; Au NRs have a flat profile (a red line). The band at 410 nm originates from the Ag center block ($L \approx 100$ nm) oscillating along the short axis of NRs (i.e., the transverse LSP mode of the Ag block). When the length of the inner Ag block increased (panels B–D) in the context of a fixed total length of heterogeneous Au–Ag–Au NRs, the band at 410 nm became more intense without noticeable peak shifts (spectra *b*, *c*, and *d*, corresponding to the samples shown in panels B, C, and D of Figure 1, respectively). The spectrum of Au (200 nm)–Ag (160 nm)–Au (200 nm) multiblock NRs has a similar profile to that of spectrum *a*. Again, there is strong LSP coupling in the long axis direction (i.e., longitudinal mode). Regardless of their relative compositions, the longitudinal LSP peak positions were determined entirely by the total length of the NRs. In our previous report on Au–Ni–Au NRs, the length of the inner component Ni required to allow longitudinal LSP coupling was restricted.^{5b} For example, when the length of the inner Ni block was 350 nm giving a total length of 550 nm, there was no longitudinal LSP coupling between the two Au blocks ($L \approx 100$ nm), and the spectrum profile of the Au–Ni–Au NR was similar to that of single-component Au NRs with a total length of $L \approx 100$ nm. This is because

[†] Department of Chemistry.

[‡] Department of Energy Science.

[§] SKKU Advanced Institute of Nanotechnology.

the free electrons on the Ni blocks could not oscillate in phase with the free electrons on the Au blocks, and they therefore acted as an inert spacer for the two Au blocks.¹³ However, in Au–Ag–Au NRs, even when the length ($L \approx 380$ nm) of the inner Ag block was much longer than the length ($L \sim 85$ nm) of the two Au blocks, the spectrum (d) of the Au–Ag–Au NR was very similar to that of Au NRs with a total length of $L \approx 550$ nm. The inner Ag block participates in the longitudinal charge density oscillation in conjunction with the two Au ends, allowing the NRs to function as a single entity. At longer wavelengths, the optical constants of Ag and Au are very similar, and therefore the peak positions of longitudinal LSP modes are determined solely by the total length of the NRs. Although the NRs behave as a single body with longitudinal LSP modes, the appearance of two transverse SP modes at 410 and 555 nm indicates independent charge oscillation of each metal block along the short axis due to the lack of coupling at shorter wavelengths. It is noteworthy that the intensity variation of higher order modes is somewhat related to the quality (surface morphology and size distribution) of NR samples rather than to the relative portion of Au and Ag blocks.

The LSP modes of metal NRs are known to depend on their aspect ratios and optical constants. To clarify the dependence of the optical properties on the aspect ratios of each block, we synthesized more complicated Au/Ag NRs composed of multisegments. The lengths of all investigated NRs were fixed to ca. 550 nm. As illustrated in Figure 2, NRs (panel A) with aspect ratios >1 for both Au and Ag blocks (with block length, $L \approx 100$ nm) were synthesized. These NRs have four boundary interfaces between the Au and Ag blocks. In panel B, Ag blocks with aspect ratios >1 but three Au blocks with an aspect ratio <1 were synthesized. In panel C, NRs with Au with an aspect ratio >1 as the major component were synthesized. The two inner Ag blocks have aspect ratios <1 . In panel D, NRs with Au and Ag blocks with aspect ratios <1 were synthesized. The corresponding UV–vis–NIR spectra of these various NRs are plotted in panel E. Although there was little difference in peak intensities, all spectra showed two transverse LSP modes from the Ag and Au domains at 410 and 555 nm, respectively. When Au was the major block in the overall nanostructure, the NR spectrum was characterized by an intensive band at 555 nm and a minor band at 410 nm (spectrum c from sample C). The opposite trend was evident when Ag was the major block (i.e., spectrum b from sample B). More importantly, longitudinal LSP modes at 740 and 1090 nm indicating higher-order modes were observed, in addition to the tail of a dipole mode around 1600 nm. This set of experiments proves that there are effective LSP couplings along the long axis of NRs and that such couplings are not limited to the aspect ratios of individual blocks and/or the number of block interfaces. The NRs shown in panel D and their corresponding spectrum d are particularly interesting. When the aspect ratios of both Au and Ag blocks are <1 , the transverse LSP modes slightly red-shift and exhibit very broad features around 550 nm due to band overlap with the longitudinal LSP mode at 740 nm. In our previous report, we found that when Ni blocks were used instead of Ag under similar morphological conditions, no longitudinal LSP mode coupling occurred.^{5b} The Ni blocks merely played the role of spacers for the Au blocks and only a single band centered at 690 nm that originated from oscillation of the Au disks along the short axis was observed, because the aspect ratio was <1 . Longitudinal LSP modes were absent from this system. However, in the current system of Au–(Ag–Au)₃ with a Au length of $L \approx 29$ nm and a Ag length of $L \approx 29$ nm, the spectrum of the sample had a similar spectral profile to those of the other three examples, with higher-order longitudinal LSP modes at 740 and 1090 nm clearly

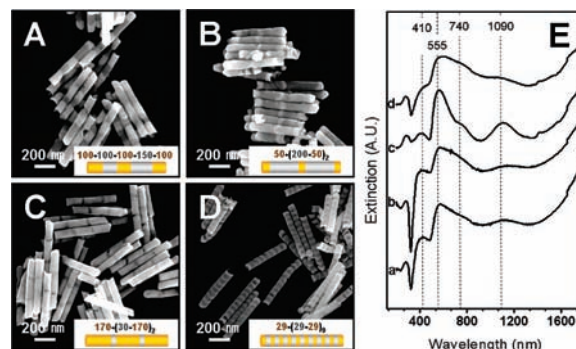


Figure 2. Similar to Figure 1, but for the different lengths and repeating units with Au and Ag blocks. The average total lengths are (A) 553 (± 42) nm, (B) 552 (± 37) nm, (C) 570 (± 41) nm, and (D) 554 (± 27) nm.

visible, as well as a long tail at 1600 nm for the dipole mode. When the total length of the NRs was fixed to 340 nm, a dipole longitudinal mode centered at 1500 nm was clearly observed (Supporting Information). These results are consistent with effective LSP coupling along the long axis of NRs.

In conclusion, we observed transverse and longitudinal LSP resonances that included higher-order modes in multiblock Au/Ag NRs. The resulting NRs had independent transverse LSP modes, but cooperative coupling of LSP modes along the long axis led to the appearance of longitudinal bands, including higher-order modes, similar to the spectral profile of single component NRs. The increased control and understanding of complicated nanostructures will lead to the design of more sophisticated plasmon waveguides and chemical and biological sensors.

Acknowledgment. This work was supported by a grant from the Korean Research Foundation funded by the Korean Government (MEST, KRF-2008-005-J00702) and grants from the Korean Science and Engineering Foundation (Nano R&D program: 2008-04285, 2008-0060482).

Supporting Information Available: Experimental details, schematic representations, FESEM images, UV–vis–NIR spectra for other NRs, and EDS mapping images. This material is available free of charge via the Internet at <http://pubs.acs.org>.

References

- (1) (a) Barnes, W. L.; Dereux, A.; Ebbesen, T. W. *Nature* **2003**, *424*, 824. (b) Oldenburg, S. J.; Jackson, J. B.; Westcott, S. L.; Halas, N. J. *Appl. Phys. Lett.* **1999**, *75*, 2897. (c) Kumbhar, A. S.; Kinnan, M. K.; Chumanov, G. *J. Am. Chem. Soc.* **2005**, *127*, 12444.
- (2) (a) Thaxton, C. S.; Mirkin, C. A. *Nat. Biotechnol.* **2005**, *23*, 681. (b) Ko, H.; Singamaneni, S.; Tsukruk, V. V. *Small* **2008**, *4*, 1576. (c) Hutter, E.; Fendler, J. H. *Adv. Mater.* **2004**, *16*, 1685. (d) Jana, N. R.; Gearheart, L.; Murphy, C. J. *J. Phys. Chem. B* **2001**, *105*, 4065. (e) Kim, F.; Song, J. H.; Yang, P. *J. Am. Chem. Soc.* **2002**, *124*, 14316.
- (3) (a) Ung, T.; Liz-Marzan, L. M.; Mulvaney, P. *J. Phys. Chem. B* **2001**, *105*, 3441. (b) Bohren, C. F.; Huffman, D. R. *Absorption and Scattering of Light by Small Particles*; John Wiley: New York, 1983.
- (4) Jain, P. K.; Eustis, S.; El-Sayed, M. A. *J. Phys. Chem. B* **2006**, *110*, 18243.
- (5) (a) Payne, E. K.; Shuford, K. L.; Park, S.; Schatz, G. C.; Mirkin, C. A. *J. Phys. Chem. B* **2006**, *110*, 2150. (b) Kim, S.; Shuford, K. L.; Bok, H.-M.; Kim, S. K.; Park, S. *Nano Lett.* **2008**, *8*, 800. (c) Bok, H.-M.; Shuford, K. L.; Kim, S.; Kim, S. K.; Park, S. *Nano Lett.* **2008**, *8*, 2265.
- (6) Khlebtsov, B. N.; Khlebtsov, N. G. *J. Phys. Chem. C* **2007**, *111*, 11516.
- (7) (a) Martin, C. R. *Science* **1994**, *266*, 1961. (b) Park, S.; Lim, J.-H.; Chung, S.-W.; Mirkin, C. A. *Science* **2004**, *303*, 348. (c) Nicewarner-Peña, S. R.; Freeman, R. G.; Reiss, B. D.; He, L.; Peña, D. J.; Walton, I. D.; Cromer, R.; Keating, C. D.; Natan, M. J. *Science* **2001**, *294*, 137. (d) Kovtyukhova, N. I.; Martin, B. R.; Mbindyo, J. K. N.; Smith, P. A.; Razavi, B.; Mayer, T. S.; Mallouk, T. E. *J. Phys. Chem. B* **2001**, *105*, 8762.

JA903093T